

Effect of thermal annealing on structural properties of GeSn thin films grown by molecular beam epitaxy

Z. P. Zhang,^{1,2,3} Y. X. Song,^{1,a} Y. Y. Li,¹ X. Y. Wu,^{1,3,5} Z. Y. S. Zhu,^{1,2}
Y. Han,^{1,3} L. Y. Zhang,¹ H. Huang,¹ and S. M. Wang^{1,2,4,a}

¹State Key Laboratory of Functional Materials for Informatics, Shanghai Institute of Microsystem and Information Technology, Chinese Academy of Sciences, Shanghai 200050, China

²School of Physical Science and Technology, ShanghaiTech University, Shanghai 201210, China

³University of Chinese Academy of Sciences, Chinese Academy of Sciences, Beijing 100190, China

⁴Department of Microtechnology and Nanoscience, Chalmers University of Technology, Gothenburg 41296, Sweden

⁵State Key Laboratory of Advanced Optical Communication Systems and Networks, Shanghai Key Laboratory on Navigation and Location-Based Service and Center of Quantum Information Sensing and Processing, Shanghai Jiao Tong University, Shanghai 200240, China

(Received 21 September 2017; accepted 19 October 2017; published online 27 October 2017)

GeSn alloy with 7.68% Sn concentration grown by molecular beam epitaxy has been rapidly annealed at different temperatures from 300°C to 800°C. Surface morphology and roughness annealed below or equal to 500°C for 1 min have no obvious changes, while the strain relaxation rate increasing. When the annealing temperature is above or equal to 600°C, significant changes occur in surface morphology and roughness, and Sn precipitation is observed at 700°C. The structural properties are analyzed by reciprocal space mapping in the symmetric (004) and asymmetric (224) planes by high resolution X-ray diffraction. The lateral correlation length and the mosaic spread are extracted for the epi-layer peaks in the asymmetric (224) diffraction. The most suitable annealing temperature to improve both the GeSn lattice quality and relaxation rate is about 500°C. © 2017 Author(s). All article content, except where otherwise noted, is licensed under a Creative Commons Attribution (CC BY) license (<http://creativecommons.org/licenses/by/4.0/>). <https://doi.org/10.1063/1.5005970>

INTRODUCTION

Group IV materials with engineered band structures have gain increased attentions in recent years.^{1,2} GeSn alloy is one of the most promising semiconductor materials with a tunable bandgap. Although Ge is an indirect bandgap semiconductor which has a 136 meV gap between the L-valley and the Γ -valley,³ introducing Sn in Ge forming a GeSn alloy could make transformation of the L-valley and the Γ -valley to convert it into a direct bandgap semiconductor. GeSn with a direct bandgap can emit light efficiently⁴ and is compatible with COMS technology.⁵⁻⁷ Noteworthy milestones like GeSn laser² have spurred a fast development in this research field. Besides the tunable bandgap, GeSn alloy is also predicted to hold high electron and hole mobility, which makes it a potential candidate material for both optoelectronic and electronic devices integrated on the Si platform.^{8,9}

The thermal equilibrium solubility of the Ge-Sn binary system is as low as 1%,¹⁰ and surface energy of Sn is smaller than that of Ge.¹¹ Therefore, Sn segregation is the largest challenge for formation of homogeneous GeSn alloys during the epitaxial growth. GeSn layers with a high Sn

^aAuthors to whom correspondence should be addressed. Electronic mail: songyuxin@mail.sim.ac.cn and shumin@mail.sim.ac.cn.

concentration have been grown by low temperature molecular beam epitaxy (MBE),¹² chemical vapor deposition^{13–16} or solid phase epitaxy.¹⁷ Moreover, some ultra-high Sn concentration GeSn alloy has been grown by MBE at a growth temperature less than 200°C, for example 25%¹⁸ and 27%.¹⁹ The non-equilibrium processes during MBE are effective to avoid Sn segregation.²⁰ However, low temperature MBE growth of GeSn alloy will introduce many defects,²¹ which are detrimental to light emission from such a material.^{18,22} Therefore, to obtain high quality and direct bandgap GeSn alloy, the dilemma between the Sn segregation at a high growth temperature and the high defect density introduced at a low growth temperature must be overcome.²³

Thermal annealing leads to decrease in defect density and improves optical quality of the GeSn alloy.²⁴ At the same time, thermal annealing could also increase the portion of substitutional Sn atoms to reduce the difficulty of realizing direct bandgap luminescence.²⁵ Previous reports have shown that when the annealing temperature of GeSn/Ge alloy is above 400°C, strain couldn't be maintained along with structure relaxation.^{24,25} Proper annealing temperature has been found to be 500°C by measuring the root mean square (RMS) roughness and average of aligned yield (from RBS)²⁶ or 550°C by using photoluminescence (PL).²³ For a partially relaxed GeSn alloy, the bandgap transition occurs when the Sn concentration is 6~11%.^{1–3,27,28} When the GeSn alloy is fully strained on a Ge substrate, the bandgap transformation from the indirect bandgap to the direct bandgap even occurs at 12%.² However, growth of high quality and high Sn concentration GeSn alloy has encountered great challenges.^{18,19} To reduce the difficulty of bandgap transformation, a feasible path is reducing or eliminating the compressive strain by thermal annealing.

In this work, 200 nm thick GeSn thin film with 7.68% Sn concentration and 25% initial strain relaxation grown by MBE has been investigated by rapid thermal annealing at different temperatures between 300–800°C. Structural properties are analyzed by two-dimensional reciprocal space mapping (2DRSM) in the symmetric (004) and asymmetric (224) planes by high resolution X-ray diffraction (XRD). The lateral correlation length (LCL) and the mosaic spread (MS) are extracted for the epi-layer peaks in the asymmetric (224) diffraction. The larger the LCL, the higher the lattice quality, while the trend for MS is opposite. Strain relaxation has also been studied by 2DRSM. The relaxation rate of the annealed GeSn alloy increases gradually when the annealing temperature is up to 600°C. The most suitable annealing temperature to improve both the GeSn lattice quality and strain relaxation rate is about 500°C.

METHODS

200 nm GeSn thin film with 7.68% Sn concentration was grown by a DCA MBE system with a base pressure of 5×10^{-10} Torr. The Ge source is an electron beam evaporator and the Sn source is an effusion cell. The absolute flux of Ge and Sn was calibrated by both electron impact emission spectroscopy and Q-pod quartz crystal monitor. Background pressure and impurities were recorded by an ultra-sensitive ion gauge and quadrupole mass spectrometer, and surface evolution during growth was monitored by *in situ* reflection high-energy electron diffraction (RHEED).

Prior to the growth, surface oxide desorption of the Ge (001) substrate was carried out by heating the substrate at 550°C for 30 min. After that, a 200 nm thick Ge buffer layer was grown to provide an atomically clean and flat surface. Then, the sample holder was cooled to 200°C and remained stable for about 5 min followed by deposit of a 200 nm thick GeSn thin film. The Ge flux was 0.75 Å/s and the Sn flux was 0.06 Å/s, and the background pressure during epitaxy was $(5-6) \times 10^{-9}$ Torr. The sample was diced into small pieces which were then rapidly annealed for 1 min at 300°C, 400°C, 500°C, 600°C, 700°C and 800°C, respectively, in a N₂ ambient condition. Surface morphology was characterized by atomic force microscopy (AFM). Structural property and Sn concentration were analyzed by 2DRSM using high resolution XRD and scanning electron microscope (SEM). Both the LCL and the MS were investigated for the epi-layer peaks in the asymmetric (224) diffraction.

RESULTS AND DISCUSSION

FIG. 1(a) shows the HRXRD (004) ω -2 θ rocking curve of the GeSn sample with 7.68% Sn concentration. The right narrow peak corresponds to the Ge substrate while the left wide peak corresponds

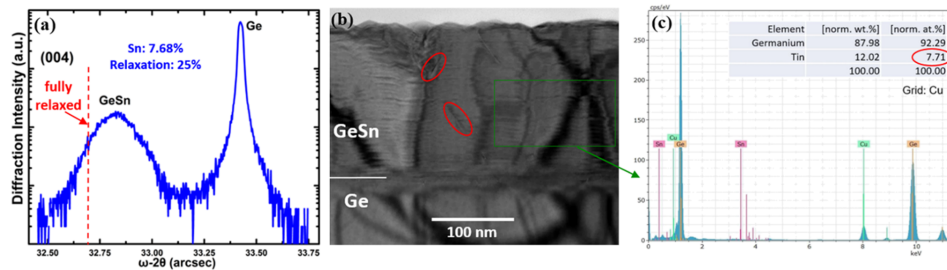


FIG. 1. (a) HRXRD (004) ω -2 θ rocking curve of the GeSn sample with 7.68% Sn concentration. (b) TEM image of the as grown sample. (c) A typical EDX spectrum of the GeSn thin film from the green rectangle area in (b).

to the GeSn epi-layer. The Sn concentration is determined by symmetric (004) and asymmetric (224) 2DRSM. The unannealed sample has a 25% initial strain relaxation rate within an experimental error of $\pm 0.2\%$. The broad epi-layer peak also indicates strain relaxation introduced by Sn incorporation. If the sample is fully strained, the peak position of the epi-layer peak should be at the red dashed line. FIG. 1(b) is a TEM image of the sample. Clear threading dislocations marked by red circles could be observed in the GeSn epi-layer, providing a proof of strain relaxation. The Sn concentration from a green rectangular area in FIG. 1(b) is listed by the red circle in FIG. 1(c) about 7.71%, in consistent with 7.68% obtained by 2DRSM.

FIG. 2(a)–(g) show SEM images of the as-grown sample and samples after thermal annealing at different temperatures. When the annealing temperature is below 600°C, there is no obvious change on surface morphology. When the annealing temperature reaches 700°C, a large number of droplets are precipitated on the surface with a density about $4.5 \times 10^6/\text{cm}^2$. Further increasing annealing temperature to 800°C, the droplet density decreases significantly to about $1.5 \times 10^6/\text{cm}^2$, while the volume of droplets increases simultaneously. FIG. 2(h) shows SEM EDX mapping of the sample annealed at 700°C, which confirms that the droplets mainly contain Sn element. When the GeSn thin film was annealed at high temperatures (above 600°C), Sn atoms can escape from the GeSn lattice sites and segregate to the sample surface, forming metallic Sn droplets. Sn segregation leads to the obvious change of surface morphology at high annealing temperatures.

FIG. 3(a)–(e) show surface morphology with increasing annealing temperature. For the as-grown sample at 200°C, the pyramid shaped features with a size of 50 nm are clearly observed with a density of $3 \times 10^9/\text{cm}^2$. FIG. 3(f) is the RMS surface roughness values extracted from the AFM images (a)–(e). With increasing annealing temperature up to 500°C, both surface morphology and roughness values are not significantly changed (at about 6 nm). However, when the annealing temperature is 600°C, the surface roughness value is reduced to 2 nm and the density of the pyramid shaped features also decreases to about $1.5 \times 10^9/\text{cm}^2$. As shown in FIG. 2(f) and (g), when the annealing temperature is

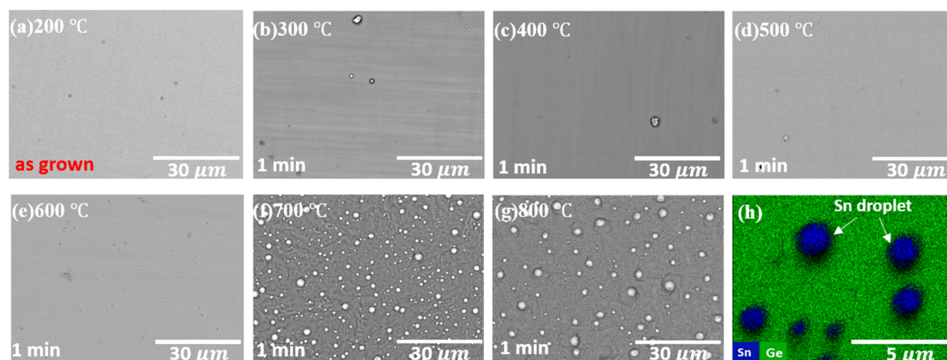


FIG. 2. SEM images of the GeSn samples after annealing at different temperatures. (a) as grown (b)–(g) after annealing at 300°C, 400°C, 500°C, 600°C, 700°C and 800°C, respectively, for 1 min; (h) SEM EDX mapping of the sample annealed at 700°C for 1 min corresponding to (f).

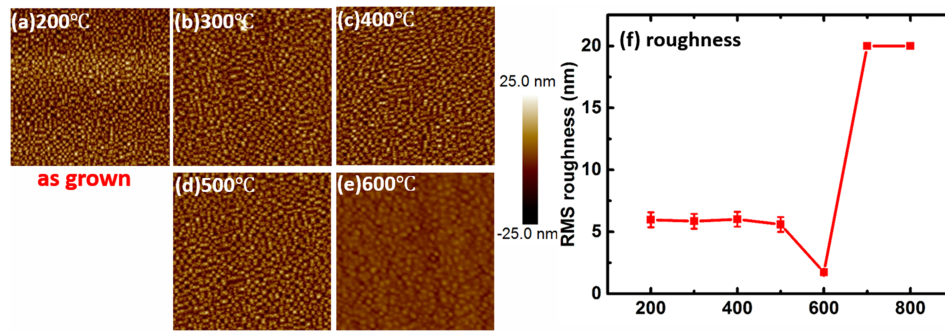


FIG. 3. $5 \times 5 \mu\text{m}^2$ AFM images of the GeSn thin films at different annealing temperatures. (a) as-grown (b)-(e) surface of the samples annealed at 300°C, 400°C, 500°C and 600°C for 1 min; (f) RMS surface roughness as a function of the annealing temperature.

700°C and 800°C, Sn droplets are precipitated on surface of the annealed sample. The RMS-value increases to 20 nm as shown in FIG. 3(f).

Structural properties and Sn concentration are analyzed by 2DRSM in the symmetric (004) and the asymmetric (224) diffraction shown in FIG. 4 by high resolution XRD. The vertical dashed-dotted line through the Ge (224) reciprocal lattice point in 2DRSM indicates the trajectory of the (224) reciprocal lattice point of a pseudomorphic growth on a Ge substrate. The diagonal dashed line through the Ge (224) point indicates the trajectory of the (224) reciprocal lattice point of a cubic structure, meaning a fully relaxed epitaxial layer. It can be observed in FIG. 4(a) that the as-grown GeSn deviates from the vertical direction, indicating onset of strain relaxation. With increase of the annealing temperature, the deviation significantly increases at 300 °C, and then slowly increases in the range of annealing temperature from 300 °C to 600 °C as shown in FIG. 4(b)–(e), which reflects the trend of strain relaxation with increasing the annealing temperature. When the annealing temperature is 700°C and 800°C, as the area indicated by the red arrow in FIG. 4(f) and (g), the separation between the substrate peak and the epi-layer peak becomes so small or almost disappear, due to the precipitation of Sn. Furthermore, peak broadening for both substrate and the epi-layer is the least at 500°C before the occurrence of Sn precipitation, indicating improvement in lattice uniformity and regularity of the GeSn alloy.

Next, by making analysis for the 2DRSM (004) and (224) plane of the annealed GeSn thin films at different temperatures, several important parameters on structural quality of GeSn have been extracted. FIG. 5(a) shows the Sn composition change with annealing temperature. When the annealing temperature is below or equal to 600°C, Sn composition is almost unchanged. But above 700°C, Sn composition decreases obviously. FIG. 5(b) shows strain relaxation is promoted with

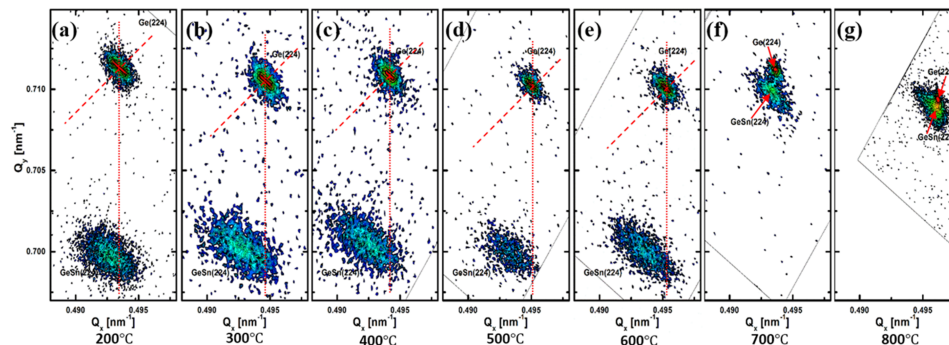


FIG. 4. XRD 2DRSM around (224) diffraction point (a) as-grown; (b)-(g) annealed at 300°C, 400°C, 500°C, 600°C, 700°C and 800°C, respectively, for 1 min. Q_x and Q_y axes are along the [110] and the [001] direction, respectively. The dashed and dashed-dotted lines indicate the fully relaxed and pseudomorphic growth, respectively.

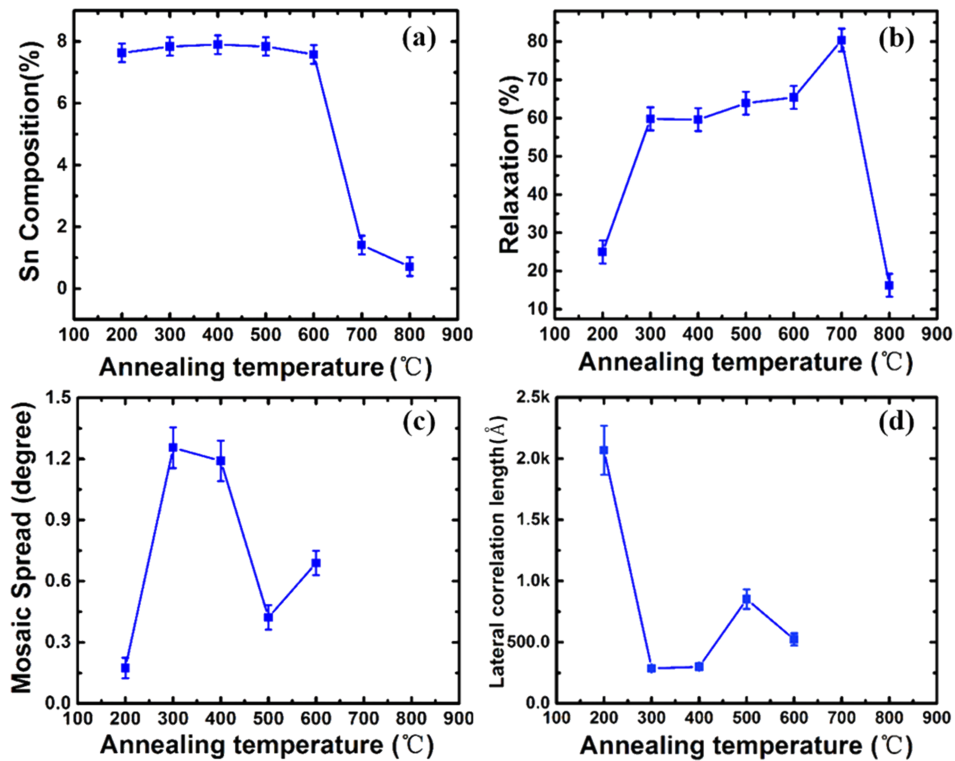


FIG. 5. (a) Sn concentration (b) strain relaxation rate (c) MS and (d) LCL extracted from the 2DRSM as a function of annealing temperature.

increasing the annealing temperature. It is observed that the as-grown GeSn sample at 200°C has a 25% initial relaxation rate. With the increase of the annealing temperature, the relaxation rate significantly increases at 300°C, and slowly rises in the range of annealing temperature from 300°C to 600°C. When the annealing temperature is 700°C and 800°C, the relaxation rate first increases and then decreases rapidly, which is probably related to the precipitation of Sn.

To further analyze crystal quality of the GeSn thin film, the MS and the LCL of the GeSn epilayers are investigated by extracting from the asymmetric (224) mapping. FIG. 5(c) and (d) separately shows the MS and the LCL change with annealing temperature. MS may arise either because of a fine mosaic structure giving a variation in the tilt of the reflecting plane for different mosaic grains or it may be a result of "rippled" reflecting planes due to the presence of a uniform dislocation density.²⁹ When lattice quality is high, the value of the MS is small conversely. FIG. 5(b) shows the relaxation rate of GeSn thin film goes up greatly after annealing at 300°C, and the reason for the increase of relaxation rate is likely from the increase of the dislocation density. Therefore, the lattice quality of the GeSn thin film is also correspondingly reduced, which is in accordance with the great increase of the MS in the annealed GeSn thin film at 300°C. LCL gives an indication of the lateral uniformity of the layer. If a layer is perfectly smooth and of uniform thickness in all directions parallel to the interface, the breadth of this peak would be related to an average value of the separation of GeSn thin film lateral irregularities.^{20,30} When lattice quality is high, the value of the LCL is also high. Therefore, FIG. 5(b)–(d) jointly indicate that 500°C is the most suitable annealing temperature to improve both the GeSn lattice quality and relaxation rate.

CONCLUSIONS

GeSn alloy with 7.68% Sn concentration grown by MBE has been rapidly annealed at different temperatures from 300°C to 800°C. The surface morphology and roughness of the samples annealed up to 500°C for 1 min have no obvious change, except for the increase in strain relaxation rate.

When the annealing temperature is above or equal to 600°C, significant changes occur in surface morphology and roughness, and Sn precipitates at 700°C. The structural properties are analyzed by reciprocal space mapping in the symmetric (004) and asymmetric (224) planes by high resolution XRD. The LCL and the MS are extracted for the epi-layer peaks in the asymmetric (224) diffraction. The most suitable annealing temperature to improve both the GeSn lattice quality and relaxation rate is about 500°C.

ACKNOWLEDGMENTS

This study was financially supported by the National Natural Science Foundation of China (61404153), the Shanghai Pujiang Program (14PJ1410600), the Key Research Program of the Chinese Academy of Sciences (KGZD-EW-804) and the Creative Research Group Project of Natural Science Foundation of China (61321492).

- ¹ S. Wirths, D. Buca, and S. Mantl, *Prog. Cryst. Growth Charact. Mater.* **62**, 1 (2016).
- ² S. Wirths, R. Geiger, N. von den Driesch, G. Mussler, T. Stoica, S. Mantl, Z. Ikonik, M. Luysberg, S. Chiussi, J. M. Hartmann, H. Sigg, J. Faist, D. Buca, and D. Grützmacher, *Nat. Photonics* **9**, 88 (2015).
- ³ S. Gupta, B. Magyari-Köpe, Y. Nishi, and K. C. Saraswat, *J. Appl. Phys.* **113**, 073707 (2013).
- ⁴ S. A. Ghetmiri, W. Du, J. Margetis, A. Mosleh, L. Cousar, B. R. Conley, L. Domulevicz, A. Nazzal, G. Sun, R. A. Soref, J. Tolle, B. Li, H. A. Naseem, and S. Q. Yu, *Appl. Phys. Lett.* **105**, 151109 (2014).
- ⁵ Y. S. Huang, Y. J. Tsou, C. H. Huang, C. H. Huang, H. S. Lan, C. W. Liu, Y. C. Huang, H. Chung, C. P. Chang, S. S. Chu, and S. Kuppuraao, *IEEE Trans. Electron Devices* **64**, 2498 (2017).
- ⁶ S. Gupta, Y. C. Huang, Y. Kim, E. Sanchez, and K. C. Saraswat, *IEEE Electron Device Lett.* **34**, 831 (2013).
- ⁷ G. Han, Y. Wang, Y. Liu, C. Zhang, Q. Feng, M. Liu, S. Zhao, B. Cheng, J. Zhang, and Y. Hao, *IEEE Electron Device Lett.* **37**, 701 (2016).
- ⁸ R. Loo, B. Vincent, F. Gencarelli, C. Merckling, A. Kumar, G. Eneman, L. Witters, W. Vandervorst, M. Caymax, M. Heyns, and A. Thean, *ECS J. Solid State Sci. Technol.* **2**, N35 (2012).
- ⁹ X. Gong, G. Han, F. Bai, S. Su, P. Guo, Y. Yang, R. Cheng, D. Zhang, G. Zhang, C. Xue, B. Cheng, J. Pan, Z. Zhang, E. S. Tok, D. Antoniadis, and Y. C. Yeo, *IEEE Electron Device Lett.* **34**, 339 (2013).
- ¹⁰ R. Chen, H. Lin, Y. Huo, C. Hitzman, T. I. Kamins, and J. S. Harris, *Appl. Phys. Lett.* **99**, 181125 (2011).
- ¹¹ L. Vitos, A. V. Ruban, H. L. Skriver, and J. Kollár, *Surf. Sci.* **411**, 186 (1998).
- ¹² S. Su, W. Wang, B. Cheng, G. Zhang, W. Hu, C. Xue, Y. Zuo, and Q. Wang, *J. Cryst. Growth* **317**, 43 (2011).
- ¹³ A. Mosleh, M. Benamara, S. A. Ghetmiri, B. Conely, M. Alher, W. Du, G. Sun, R. Soref, J. Margetis, J. Tolle, S.-Q. Yu, and H. Naseem, *ECS Trans.* **64**, 895 (2014).
- ¹⁴ J. Aubin, J. M. Hartmann, L. Milord, V. Reboud, A. Gassenq, N. Pauc, and V. Calvo, *J. Cryst. Growth* **473**, 20 (2017).
- ¹⁵ B. Vincent, F. Gencarelli, H. Bender, C. Merckling, B. Douhard, D. H. Petersen, O. Hansen, H. H. Henriksen, J. Meererschaut, W. Vandervorst, M. Heyns, R. Loo, and M. Caymax, *Appl. Phys. Lett.* **99**, 152103 (2011).
- ¹⁶ F. Gencarelli, B. Vincent, L. Souriau, O. Richard, W. Vandervorst, R. Loo, M. Caymax, and M. Heyns, *Thin Solid Films* **520**, 3211 (2012).
- ¹⁷ R. R. Lieten, J. W. Seo, S. Decoster, A. Vantomme, S. Peters, K. C. Bustillo, E. E. Haller, M. Menghini, and J. P. Locquet, *Appl. Phys. Lett.* **102**, 052106 (2013).
- ¹⁸ M. Oehme, K. Kosteci, M. Schmid, F. Oliveira, E. Kasper, and J. Schulze, *Thin Solid Films* **557**, 169 (2014).
- ¹⁹ M. Nakamura, Y. Shimura, S. Takeuchi, O. Nakatsuka, and S. Zaima, *Thin Solid Films* **520**, 3201 (2012).
- ²⁰ Z. P. Zhang, Y. X. Song, Z. Y. S. Zhu, Y. Han, Q. M. Chen, Y. Y. Li, L. Y. Zhang, and S. M. Wang, *AIP Adv.* **7**, 045211 (2017).
- ²¹ O. Nakatsuka, N. Taoka, and T. Asano, *ECS Trans.* **58**, 149 (2013).
- ²² R. Hickey, N. Fernando, S. Zollner, J. Hart, R. Hazbun, and J. Kolodzey, *J. Vac. Sci. Technol. B* **35**, 021205 (2017).
- ²³ N. Taoka, G. Capellini, V. Schlykow, M. Montanari, P. Zaumseil, O. Nakatsuka, S. Zaima, and T. Schroeder, *Mater. Sci. Semicond. Process.* **57**, 48 (2017).
- ²⁴ H. Li, Y. X. Cui, K. Y. Wu, W. K. Tseng, H. H. Cheng, and H. Chen, *Appl. Phys. Lett.* **102**, 251907 (2013).
- ²⁵ C. M. Comrie, C. B. Mtshali, P. T. Sechogela, N. M. Santos, K. Van Stiphout, R. Loo, W. Vandervorst, and A. Vantomme, *J. Appl. Phys.* **120**, 145303 (2016).
- ²⁶ X. Zhang, D. Zhang, B. Cheng, Z. Liu, G. Zhang, C. Xue, and Q. Wang, *ECS Solid State Lett.* **3**, P127 (2014).
- ²⁷ D. Stange, S. Wirths, N. Von Den Driesch, G. Mussler, T. Stoica, Z. Ikonik, J. M. Hartmann, S. Mantl, D. Grützmacher, and D. Buca, *ACS Photonics* **2**, 1539 (2015).
- ²⁸ C. L. Senaratne, J. D. Gallagher, T. Aoki, J. Kouvetakis, and J. Menéndez, *Chem. Mater.* **26**, 6033 (2014).
- ²⁹ P. Fini, H. Marchand, J. P. Ibbetson, S. P. DenBaars, U. K. Mishra, and J. S. Speck, *J. Cryst. Growth* **209**, 581 (2000).
- ³⁰ R. Schad, P. Beliën, G. Verbanck, V. V. Moshchalkov, Y. Bruynseraede, H. E. Fischer, S. Lefebvre, and M. Bessiere, *Phys. Rev. B* **59**, 1242 (1999).